Comparison of HII, HIII and THOR dummy responses with respect to PMHS sled tests

Jérôme Uriot, Pascal Potier, Pascal Baudrit, Xavier Trosseille, Olivier Richard, Richard Douard

Abstract Nine Post Mortem Human Subject (PMHS) tests were published by Luet et al. (2012) as a reference for submarining assessment. These tests suffered limitations, however, due to the rigid characteristics of the seat. The objective of this study is to assess the submarining ability of existing dummies in more realistic conditions, i.e. on a real seat.

In total, nine PMHS sled tests were performed on a real seat to procure data in 3 different configurations. The tests were also duplicated with HII, HIII and THOR Mod Kit dummies to evaluate their behaviour in comparison to corridors built with 3 PMHS each.

The external forces, the pelvis kinematics and the injury assessments are provided here. The dummy responses are compared to the PMHS corridors. No submarining was observed in the standard configuration. Iliac crest fractures and submarining were observed in the slouched position intended to generate submarining. Finally, for two subjects out of three, no iliac wing fracture and no submarining were observed in the slouched position with a lap-belt load limitation at 4 kN and a pretension system.

Keywords frontal test, lap-belt, pelvis, PMHS, submarining.

I. INTRODUCTION

Although the submarining process began to be studied in the 1970s, few data are available at this time to evaluate the ability of surrogates to mimic this phenomenon. Moreover, the studies were carried on commercial seats 30 years ago, compromising the possibility of reproducing them to evaluate current dummies. Finally, the pelvis kinematics was not measured. To address these drawbacks, Luet et al. [1] published tests carried out with 9 PMHS in 3 configurations as a reference for submarining assessment. These tests suffered limitations, however, due to the rigid characteristics of the seat. The objective of this study is to assess the submarining ability of existing dummies in more realistic conditions, i.e. on a real seat. They were also a mean to validate the predictions made by a modified model of the THOR NT dummy, presented in a companion paper by Richard et al. [2].

II. METHODS

For that purpose, new tests were performed on a real seat to procure data in 3 different configurations: first, in a standard position; then, in a slouched position intended to generate submarining; and finally, in a slouched position, but with a lap-belt load limitation. The same tests were also performed with HIII and THOR Mod Kit dummies to evaluate their behaviour in comparison to corridors built with 3 PMHS each. HII tests were also performed in the slouched configuration.

Except for the seat, the belt arrangement and the pulse, the test protocol was the same as in [1].

J. Uriot, P. Potier and P. Baudrit work at CEESAR, France. X. Trosseille (e-mail: xavier.trosseille@lab-france.com) works at LAB PSA Peugeot-Citroën Renault, France. O. Richard works at Faurecia Automotive Seating, France. R. Douard works at Université Paris Descartes, France.

Lumbar spine and abdomen static behaviour characterisation

The subjects were first tested for lumbar spine and abdomen quasi-static response in flexion and extension (Fig. 1). The thighs and the pelvis were secured on a rigid seat by means of external plates, screws and a lap belt. The thorax was secured to a mobile arm by means of belts. The rigid seat was fixed to the ground through a transducer measuring the moment along a Y-axis passing through the sacral plateau. The mobile arm rotated around the same axis. The pelvis and the T12 vertebrae were equipped with tilt sensors providing their angular position during the test. The thorax was bent forward and backward up to a 30 Nm moment measured at the level of the sacral plateau. This bench allowed for the caracterisation of the combined lumbar spine and abdomen angular behaviour at S1 level.

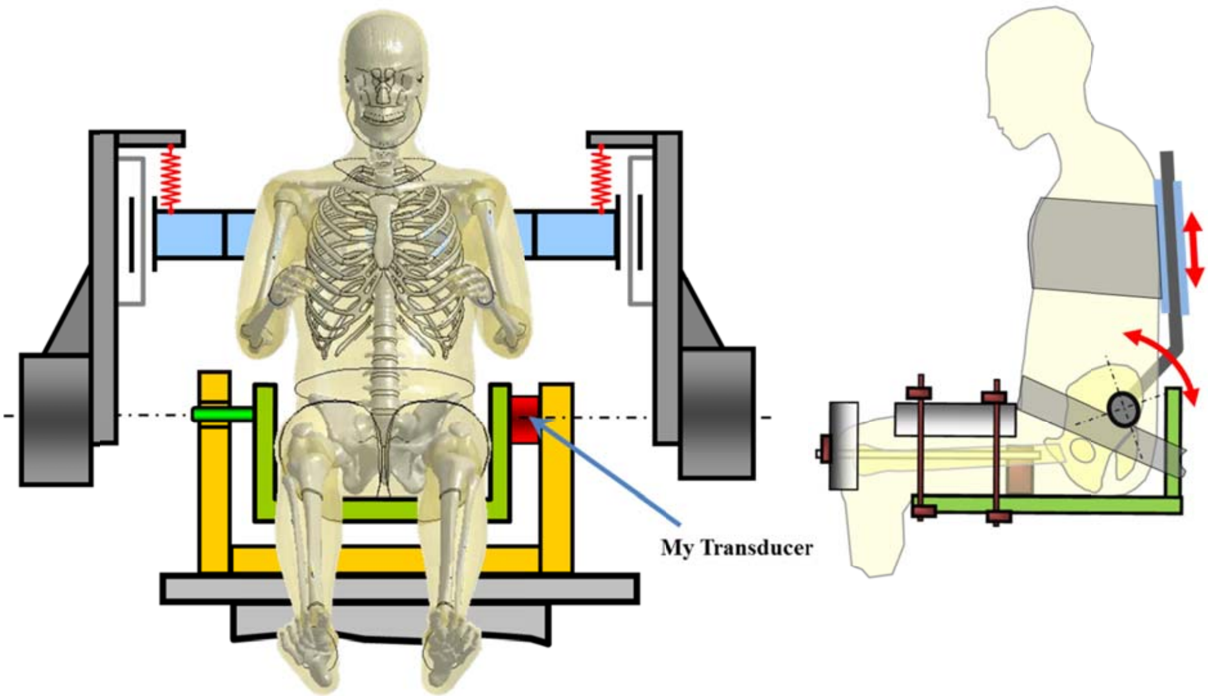

Fig. 1. Lumbar spine and abdomen static test setup.

Sled test set-up and matrix

The subjects were tested on a sled in 3 configurations:

- the first configuration consisted of a standard seat with a standard three-point belt. The subjects were seated in a standard passenger position. The shoulder-belt was equipped with a load limitation device set at 6 kN and a pyrotechnic retractor.
- The second configuration was the same as the first one, except that the subjects were seated in a slouched position. To achieve this position, the pelvises of the subjects were pushed forward by 60 mm from the standard position. In addition, the seat was moved forward by 50 mm. The pretension was not activated.
- In the third configuration, the subject was seated as in configuration 2. The shoulder-belt and the lap-belt were separated. The upper shoulder-belt force was limited at 6 kN and the lap-belt force at 4 kN. The lap-belt was equipped with two pyrotechnic retractors.

The same pulse was used for all the tests (Fig. 2). The final velocity was 14 m/s.

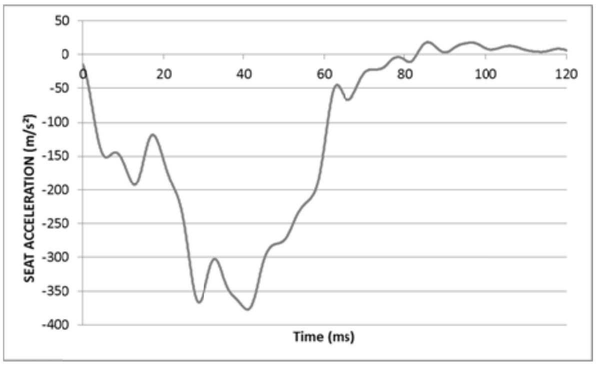

Fig. 2. Pulse.

Instrumentation

The seat was equipped with a 6-axis load cell. The upper shoulder-belt and the outboard lap-belt were fixed to the bench through 3-axis load cells. The lap-belt angle was measured with an angular velocity sensor. 3-axis accelerations were measured at T1, T12 and sacrum on the subjects. In addition, y-axis angular velocity sensors were fixed at T1 and sacrum level. All the channels were filtered CFC180, except the seat forces and sled accelerations filtered CFC60.

The coordinate system was defined in accordance with SAE J211 specifications [3]. The longitudinal x-axis was directed forward, the y-axis left-to-right and the vertical z-axis downward. As a consequence, rearward rotations of the pelvis are positive.

Surrogates

The nine PMHS were provided by Body Donations to Science at the University of Medicine René Descartes in Paris, after approval of the experimental procedure by the Ethics Committee of that University. All PMHS were un-embalmed and screened for Hepatitis C virus (HCV), Hepatitis B virus (HBV), Human Immunodeficiency Virus (HIV), Cytomegalovirus (CMV) and Human Tlymphotropic viruses (HTLV). A medical survey was documented such that any PMHS suspected of bone fragility resulting from a long bed stay, bone cancer or metastasis was excluded.

PMHS characteristics are provided in Table I. They were selected to form 3 groups of approximately the same means of age, mass, size and Body Mass Index (BMI).

TABLE I
PMHS CHARACTERISTICS AND GROUPING

PMHS	Gender	Age	Mass (kg)	Height (cm)	BMC	Group
IRIS32-MS649	M	80	81.5	178	25.7	Standard
IRIS33-MS650	M	60	68.5	176	22.1	
IRIS34-MS648	M	76	73	174	24.1	
Mean		72	74.3	176	24.0	
IRIS29-MS653	M	75	57.5	168	20.4	Slouched
IRIS30-MS652	M	63	70	180	21.6	
IRIS31-MS651	M	68	80.5	176	26	
Mean		68.7	69.3	175	22.7	
IRIS39-MS659	M	70	54	167	19.4	Prototype
IRIS40-MS657	M	88	90.5	178	28.6	
IRIS41-MS658	M	64	69	179	21.5	
Mean		74	71.2	175	23.2	

III. RESULTS

Positioning

Table II summarises the positioning of the 9 PMHS. All the angles are expressed with respect to the vertical axis.

TABLE II
PMHS POSITIONING

		Pelvis angle (deg.)		**Outboard Lap-belt angle**	**H point coordinate (mm)**		**Femur angle**	**Tibia angle**
		Nyquist plane	**Crest line**	**(deg.)**	**X**	**Z**	**(deg.)**	**(deg.)**
Standard config.	IRIS 32 - MS649	34.7	6.3	-39	132.9	-269.6	-66	41.7
	IRIS 33 - MS650	39.8	20.7	-38	158	-281.3	-68.5	35
	IRIS 34 - MS648	25.4	-9.5	-34	130.7	-277	-68.8	41.4
	Average	**33.3**	**5.8**	**-37**	**140.5**	**-276.0**	**-67.8**	**39.4**
	St. dev.	7.3	15.1	2.6	15.2	5.9	1.5	3.8
Slouched config.	IRIS 29 - MS653	59.7	9.6	-50	250.8	-296.3	-63.7	27
	IRIS 30 - MS652	61	30.9	-45	279.1	-315.6	-59.9	20.5
	IRIS 31 - MS651	59.8	30.8	-43	281	-315	-60.2	23.5
	Average	**60.2**	**23.8**	**-46**	**270.3**	**-309.0**	**-61.3**	**23.7**
	St. dev.	0.7	12.3	3.6	16.9	11.0	2.1	3.3
Prototype config.	IRIS 39 - MS659	50.3	24	-27	244	-310	72.2	45.8
	IRIS 40 - MS657	66.7	52.3	-34	251	-305	60.7	28.4
	IRIS 41 - MS658	52	36.8	-28	228.5	-298.5	65.5	25.5
	Average	**56.3**	**37.7**	**-30**	**241.2**	**-304.5**	**66.1**	**33.2**
	St. dev.	9.0	14.2	3.8	11.5	5.8	5.8	11.0

Lumbar spine and abdomen flexion tests

Fig. **3** compares the moment-angle responses of the 9 PMHS together with the HII, HIII and THOR dummy responses. While the PMHS responses are rather spread (mean of 13.5 degrees and standard deviation of 6 degrees at 25 Nm), the dummy responses are outside their range (respectively, 3.5, 1.7 and 2.8 degrees at 25 Nm for the HII, HIII and THOR dummies).

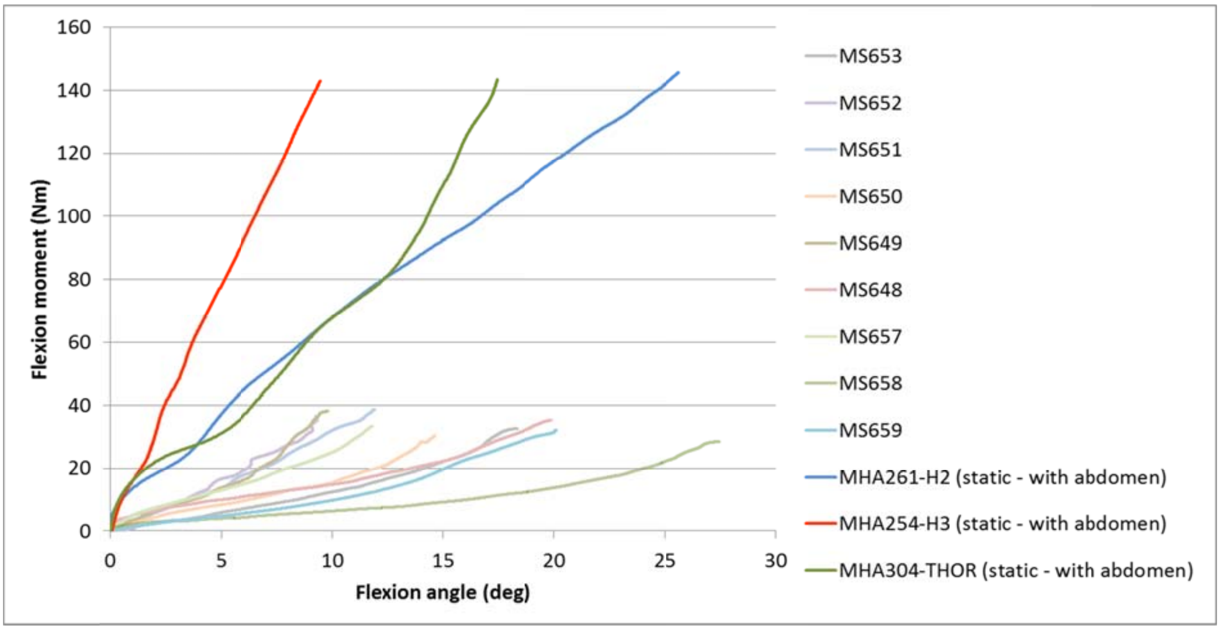

Fig. 3. Moment-angle response of lumbar spines and abdomens in flexion.

Submarining

Submarining occurred in the 3 PMHS tests of the slouched configuration, around 50 ms (47, 49 and 57 ms). It was detected on the film as the movement of the lap-belt over the iliac crest into the abdomen. No submarining was observed either in the standard position or with the prototype configuration. Concerning the dummies, the HIII dummy never submarined. In the slouched configuration, the THOR Mod Kit dummy submarined between 48 ms (on the left side) and 55 ms (on the right side) and the HII dummy submarined at 58 ms. In the Prototype configuration, the submarining of the THOR dummy was unclear, with no evidence on the film and only a slow decrease of the left ASIS forces, but no drop.

TABLE III
SUBMARINING RESULTS: OBSERVATION AND TIMING

		Submarining (Y/N)	Submarining time (ms)
Standard configuration	IRIS32-MS649	N	-
	IRIS33-MS650	N	-
	IRIS34-MS648	N	-
	IRIS35-HIII	N	-
	IRIS47-THOR	N	-
Slouched configuration	IRIS29-MS653	Y	57
	IRIS30-MS652	Y	49
	IRIS31-MS651	Y	47
	IRIS28-HII	Y	58
	IRIS36-HIII	N	-
	IRIS46-THOR	Y	48 right – 55 left
Prototype configuration	IRIS39-MS659	N	-
	IRIS40-MS657	N	-
	IRIS41-MS658	N	-
	IRIS38-HIII	N	-
	IRIS45-THOR	unclear	Decrease of left ASIS @45ms

Dynamics and kinematics

Measurement problems were encountered with IRIS29-MS653. Consequently, this subject will not appear in the time history curves.

The main results dealing with submarining, i.e. forces applied to the pelvis and pelvis kinematics, are presented in Fig. 4–8. The other parameters are provided in Appendix B–D.

It can be observed that PMHS fall into rather narrow corridors, except for the pelvis rotation. The HII and HIII dummies had higher lap-belt forces, seat forces and pelvis accelerations than the PMHS and the THOR Mod Kit dummy in the slouched configuration. In the other configurations, the THOR Mod Kit dummy had lower forces and pelvis accelerations than the HIII dummy, but both dummies were close to the PMHS.

The HIII dummy had always smaller pelvis rotations than the THOR Mod Kit dummy, but both were close to the PMHS corridors (except for the prototype configuration where the THOR Mod Kit dummy was clearly outside). In the slouched configurations, the HII demonstrated higher pelvis rotations than all other surrogates. The belt Y-rotations were close to each other for the 3 dummies and the PMHS, except for the prototype configuration where the HIII dummy rotation rises earlier. In this configuration, the belt rotations were higher with the HIII and THOR Mod Kit dummies than with the PMHS. Finally, for the HIII dummy, the pelvis to belt Y-rotation was in the PMHS corridor in the standard configuration, under the PMHS corridor in the slouched configuration (before the PMHS submarining) and above the corridor in the prototype configuration. For the THOR Mod Kit dummy, the pelvis to belt Y-rotation was above the corridors in the standard and prototype configuration and within the corridor in the slouched configuration. The HII dummy demonstrated too high rotations in the slouched configuration.

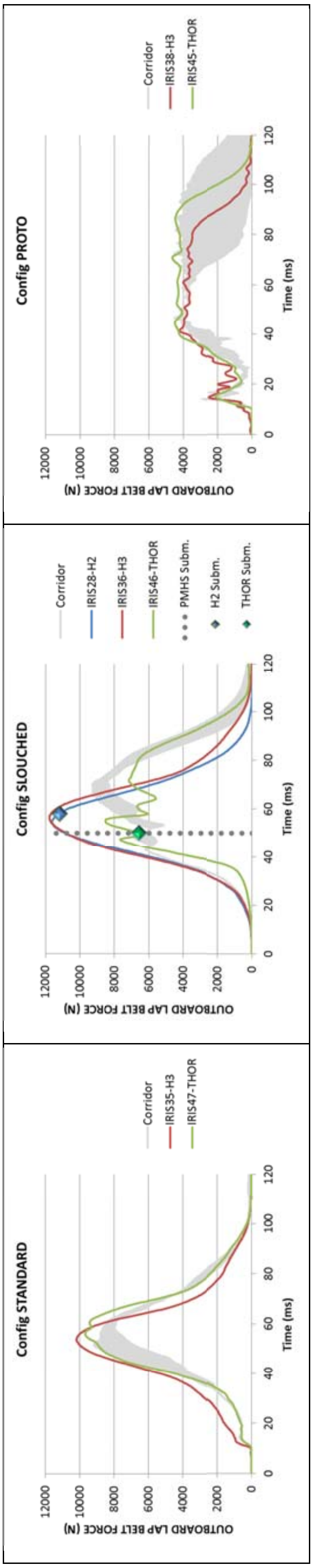

Fig. 4. Outboard Lap-belt Forces.

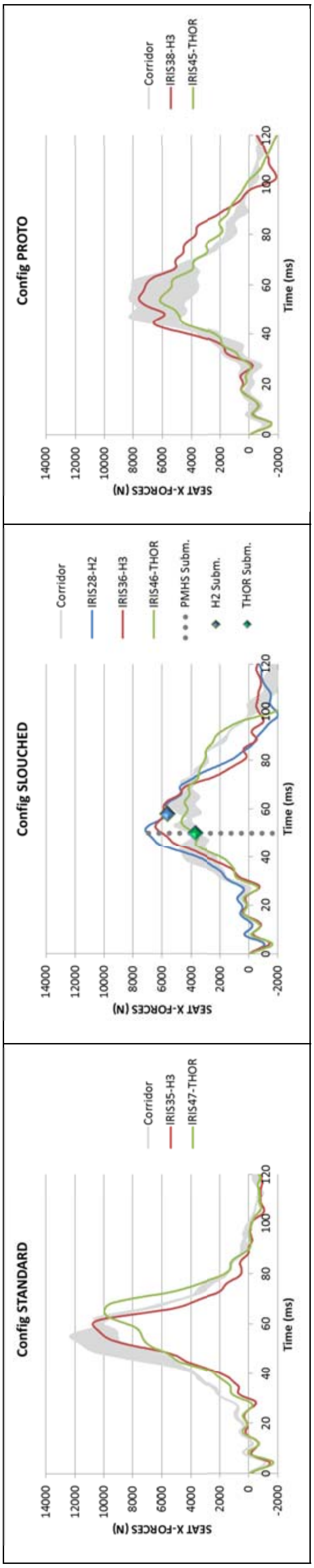

Fig. 5. Seat X Forces.

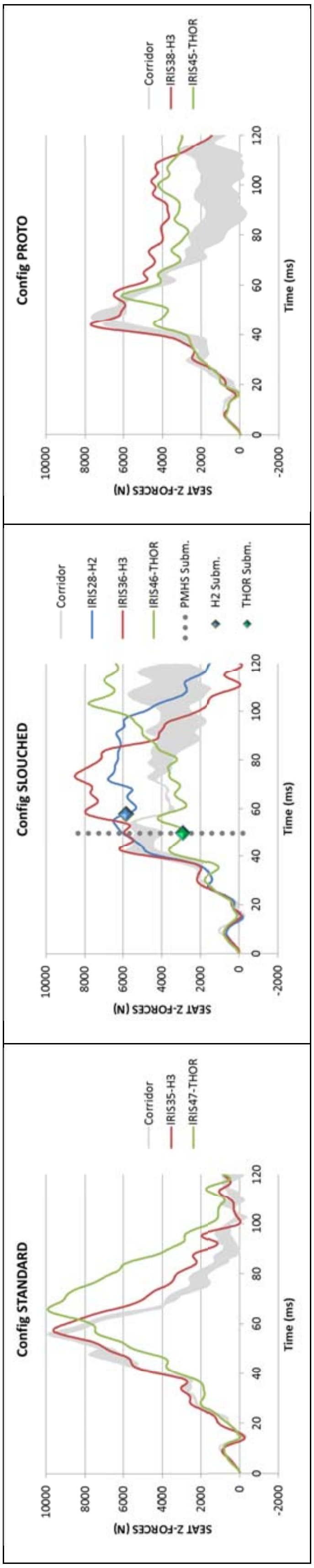

Fig. 6. Seat Z Forces.

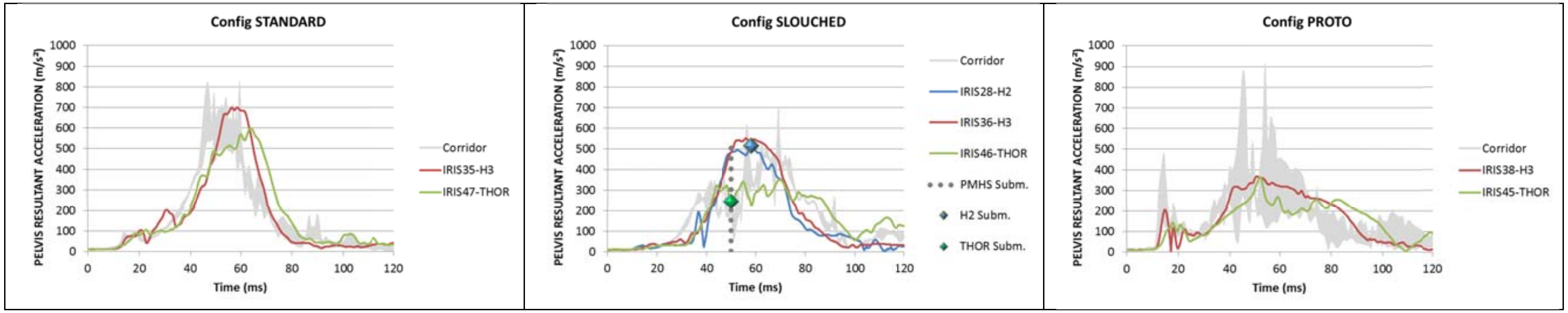

Fig. 7. Pelvis Resultant acceleration.

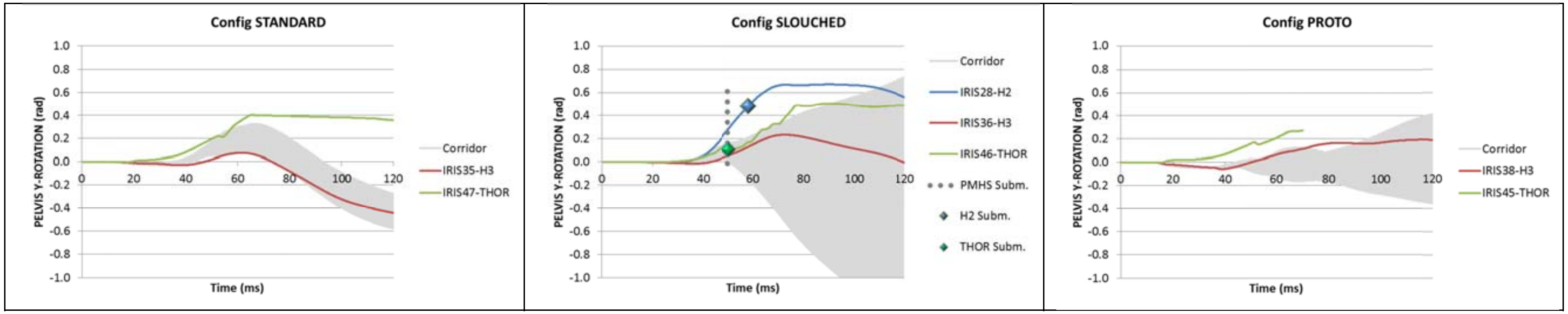

Fig. 8. Pelvis Y-rotation.

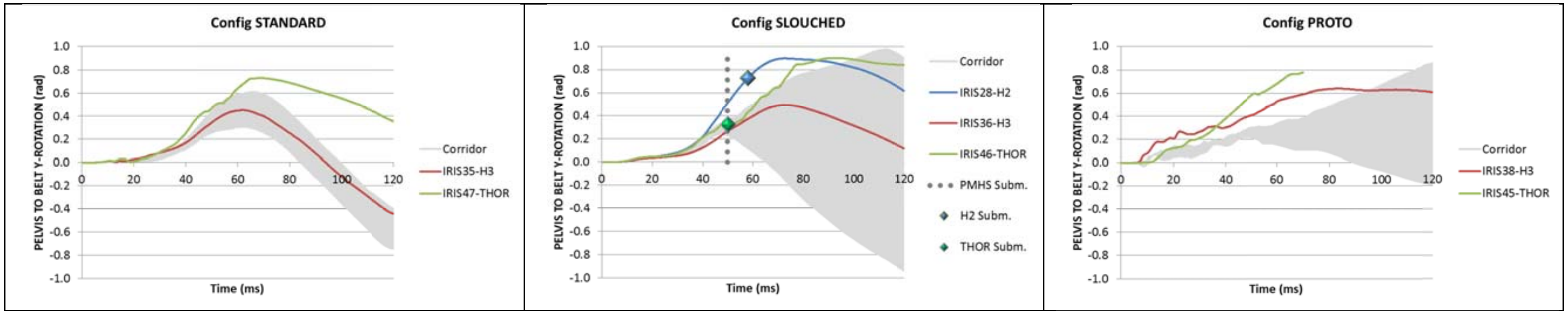

Fig. 9. Pelvis to Belt Y-rotation.

Injuries

Table A 1 summarises thorax injuries. The AIS ranges from 3 to 5 on all the subjects, with multiple rib fractures.

Table A 2 summarises pelvis, abdomen and lumbar spine injuries. The “time of fracture” indicated in this table comes from the analysis of strain gages glued on the iliac wings and on the five lumbar vertebral bodies. Fig. 10 shows the pelvic fracture localisation on the nine subjects.

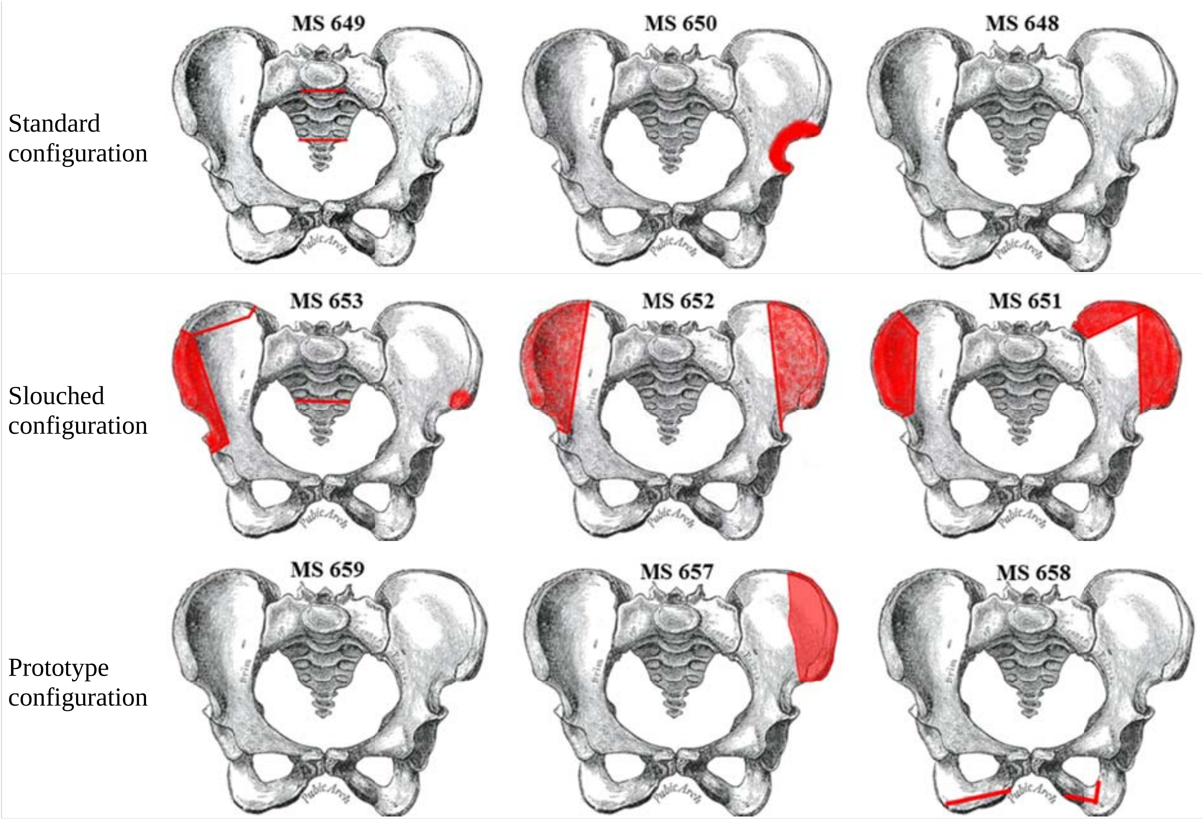

Fig. 10. Localisation of pelvis fractures.

Table IV provides the outboard lap-belt forces at the time of iliac spine fracture as well as the maximum outboard lap-belt forces.

TABLE IV
ILIAC SPINE FRACTURES AND OUTBOARD LAP-BELT FORCES

		Time of Iliac spine Fracture (ms)	Outboard lap-belt force @ fracture (N)	Maximum outboard lap-belt force (N) and time (ms)
Standard configuration	IRIS32-MS649	-	-	9217@51.8
	IRIS33-MS650	70.5	4844	7911@58.5
	IRIS34-MS648	-	-	8850@55.1
Slouched configuration	IRIS29-MS653	58.5	3987	7425@47.2
	IRIS30-MS652	50	6216	8326@71.0
	IRIS31-MS651	48.5	6752	9334@69.2
Prototype configuration	IRIS39-MS659	-	-	4270@47.7
	IRIS40-MS657	94	4205	4593@46.7
	IRIS41-MS658	-	-	4122@46.9

IV. DISCUSSION

Submarining and iliac wing fractures

All PMHS sustained iliac wing fractures at about 50 ms in the slouched configuration. IRIS40-MS657 also sustained such a fracture, but very late, at 94 ms. This is a limitation of the study, where it was not possible to dissociate iliac wing fractures from submarining. This was also the case in [1] and [4]. However, the signal of the strain gages glued on the iliac bone indicated that both phenomena were very close to each other, submarining occurring just before fracture in some cases and just after in other cases. Iliac wing fractures require a high load with a belt positioned high on the pelvis, close to the Antero-Superior Iliac Spine (ASIS). In the standard configuration, the lap-belt stays low on the pelvis, with a low Nyquist plane initial angle (33 degrees), a low lap-belt initial angle (-37 degrees) and 23 degrees of pelvis to belt rotation at the maximum lap-belt force. High loads were measured (8660 N as a mean), but no major iliac wing fractures were observed. In the slouched configuration, with a high Nyquist plane initial angle (60 degrees), a high lap-belt initial angle (-46 degrees) and 17 degrees of pelvis-to-belt rotation, the lap-belt slipped to the ASIS. In that case, major iliac wing fractures appeared at lap-belt forces between 3987 and 6752 N.

Submarining assessment

The straightforward assessment of dummies, or models' biofidelity in terms of submarining, is to check if these surrogates behave like PMHS or not in different configurations. From this point of view, if we consider this test series, the HIII dummy did not predict submarining in the slouched configuration, while the HII and the THOR Mod Kit dummies did. Moreover, the THOR Mod Kit dummy better predicts the time of submarining. In [1], however, it was found that the HII dummy submarined too easily but better predicted the time of submarining than the HIII dummy. Only looking at the occurrence and time of submarining is not enough to evaluate the biofidelity of the dummies, because the conclusions may depend on the test configuration. Therefore, a more detailed analysis is required, which evaluates the biofidelity of each component leading to submarining. Since each component interacts with the others it is quite difficult to interpret the different effects, and simulations would be of great help.

Lumbar spine and abdomen stiffness

Fig. **3** shows that the lumbar spine and abdomen of all the dummies is far too stiff. This is a key factor explaining the difference between the HII and the HIII since the pelvis of the two dummies is the same.

The THOR Mod Kit dummy is close to the HII dummy up to 80 Nm, but stiffens after, as for the HIII dummy. This allows easier rotations of the pelvis in relation to the thorax for small movements, but then rotations become more difficult, as for the HIII dummy. It has to be noted, however, that moment angle curves are not available for PMHS after 30 Nm. Moreover, only the quasi-static behaviour was tested and the difference between the PMHS's and the dummies may not be the same in dynamic conditions.
The lumbar spine was not tested alone, but in combination with the abdomen, which may have a substantial contribution to the overall behaviour. The balance between the two contributions may be different for the PMHS's and the dummies, leading to different contributions to the pelvis dynamics.

Limitations

The tests presented in this document are not easily reproducible because of the unpublished data of the real seat. However, they provide information on the behaviour of existing dummies against PMHS in actual configurations. Besides, they provide responses in realistic configurations, which can be mimicked by more reproducible means.

V. CONCLUSIONS

Nine PMHS sled tests were performed to provide data related to submarining. They allow for the evaluation of human surrogates in terms of pelvis kinematics and dynamics. While not fully reproducible, they can be used as a reference to develop further, more controlled tests.

VI. ACKNOWLEDGEMENTS

This study could not have been realised without the gift of body donors, through the Body Donation to Science centre of the University René Descartes in Paris Vth.

The authors would like also to thank Stéphane Leger from Faurecia Automotive Seating, Catherine Potier, Gilles Daniel, Denis Dubois, David Loury and Matthieu Lebarbé from CEESAR for their contribution to the tests and for their analysis.

VII. REFERENCES

[1] Luet, C., Trosseille, X., Drazétic, P., Potier, P., Vallancien, G. Kinematics and Dynamics of the Pelvis in the Process of Submarining using PMHS Sled Tests. *Stapp Car Crash Journal*, 2012, Vol. 56:411–442.

[2] Richard, O., Uriot, J., Trosseille, X., Sokolowski, M. Occupant restraint optimization in frontal crash to mitigate the risk of submarining in out of position situation. *Proceedings of IRCOBI Conference*, 2015, Lyon (France).

[3] Society of Automotive Engineers (2007) SAE J 211-1: Instrumentation for Impact Test - Part 1 - Electronic Instrumentation, Society of Automotive Engineers.

[4] Uriot, J., Baudrit, P., et al. Investigations on the Bet-to-Pelvis Interaction in Case of Submarining. *Strapp Car Crash Journal*, 2006, Vol. 50:53–73.

VIII. APPENDIX

Appendix A: Injuries

TABLE A 1
THORACIC INJURIES

	Test number	MAIS 2005	Thorax stability	Sternum Fracture	NSFR*	NSRF*	NFR**	NRF**
Standard	IRIS32-MS649	4	na	1	14	20	15	25
	IRIS33-MS650	4	na	1	3	3	11	15
	IRIS34-MS648	3	na	1	13	19	13	21
Slouched	IRIS29-MS653	5	na	1	18	32	19	36
	IRIS30-MS652	3	na	1	19	23	19	35
	IRIS31-MS651	4	na	2	20	31	20	35
Proto	IRIS39-MS659	3	Left instability	1	6	8	12	22
	IRIS40-MS657	3	Right instability	2	12	20	14	28
	IRIS41-MS658	3	Instability	1	11	12	14	27

* Number of Separated Fractured Ribs or Rib Fractures.
** Number of Fractured Ribs or Rib Fractures, including cartilage fractures.

TABLE A 2
PELVIS, ABDOMEN AND SPINE INJURIES WITH THEIR 2005 AIS AND TIME OF FRACTURE

Config.		Description of injuries	MAIS 2005	Time of fracture (ms)
Standard	IRIS 32	Fracture with displacement at S1 and S5.	2	53
	MS649	Multiple abdominal injuries.	3	
		No spine injury.	0	
	IRIS 33	Crush fracture of the anterior part of the left iliac wing.	1	70.5
	MS650	Colon injury.	3	
		No spine injury.	0	
	IRIS 34 MS648	Bilateral dilacerations of the gluteus minimus and medius muscles.	1	
		Spleen abrasion.	2	
		No spine injury.	0	
Slouched	IRIS 29	Left and Right iliac wing fractures. Sacrum fracture.	2	58.5
	MS653	Multiple abdominal injuries.	3	
		Full fracture of L4 vertebral body.	3	52
	IRIS 30	Left and Right iliac wing fractures.	2	50
	MS652	Mesentera laceration.	2	
		No spine injury.	0	
	IRIS 31	Left and Right iliac wing fractures.	2	48.5
	MS651	Colon injury.	3	
		No spine injury.	0	
Proto	IRIS 39 MS 659	Bilateral dilacerations of the gluteus minimus and medius muscles.	1	
		Severe liver injury.	5	
		Major compression fracture with dislocation of T12 vertebrae.	3	80
	IRIS 40	Left iliac wing fracture.	2	94
	MS 657	Little capsular tear of the spleen.	2	
		No spine injury.	0	
	IRIS 41	Fracture of the left and right ischio-pubic archs.	2	60
	MS 658	Multiple abdominal injuries.	5	
		No spine injury.	0	

Appendix B: Surrogate/environment interaction

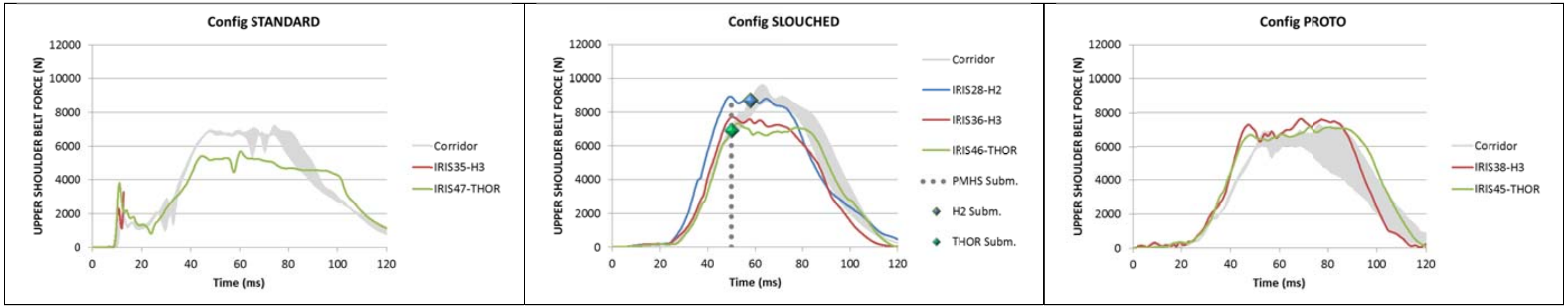

Fig. B 1. Upper Shoulder-belt Forces.

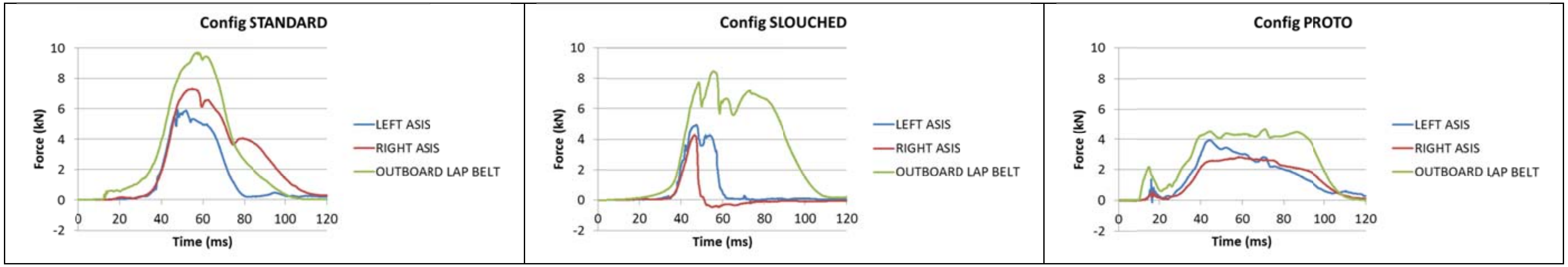

Fig. B 2. ASIS Forces for THOR Mod Kit.

Appendix C: Surrogates' kinematics

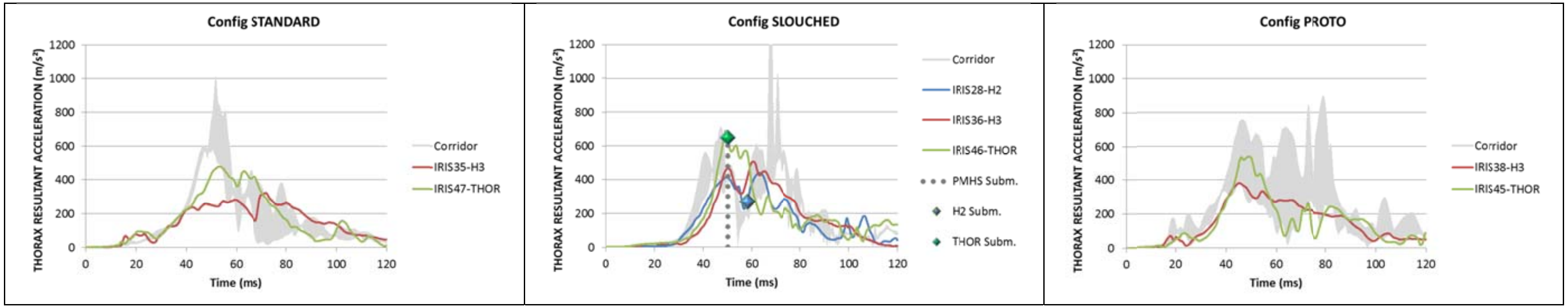

Fig. C 1. Thorax Resultant Acceleration.

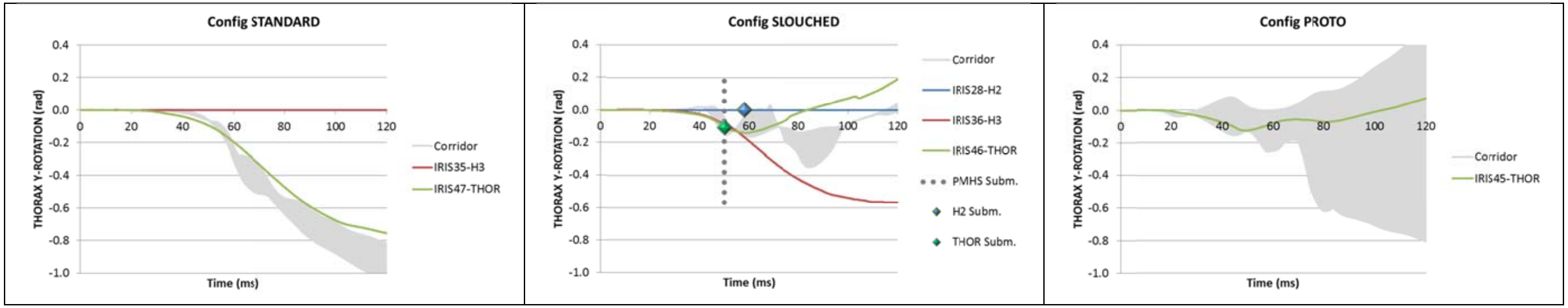

Fig. C 2. Thorax Y-Rotation.

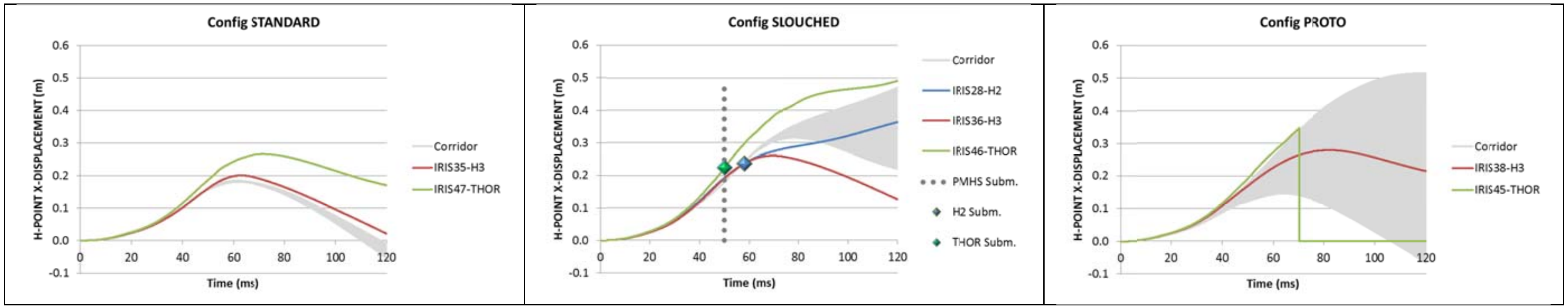

Fig. C 3. H-point X Displacement.

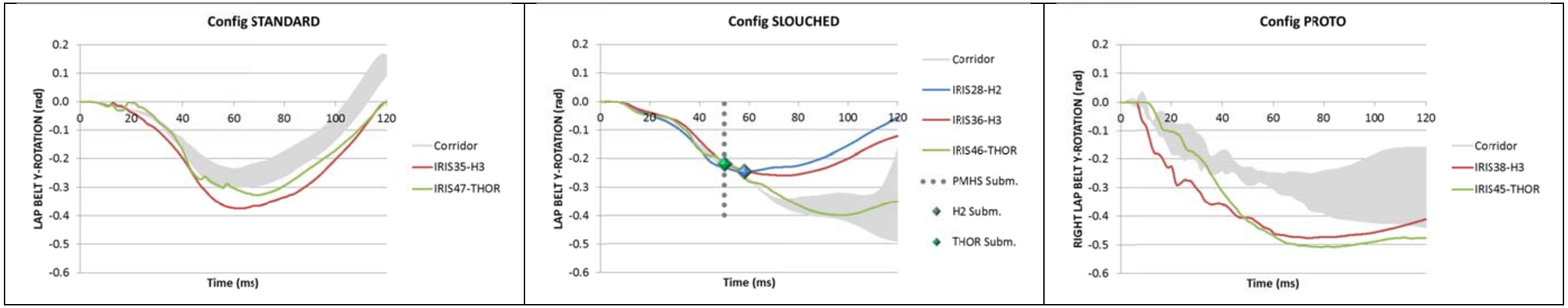

Fig. C 4. Lap-belt Y-Rotation.

Appendix D: Lumbar Spine Loads

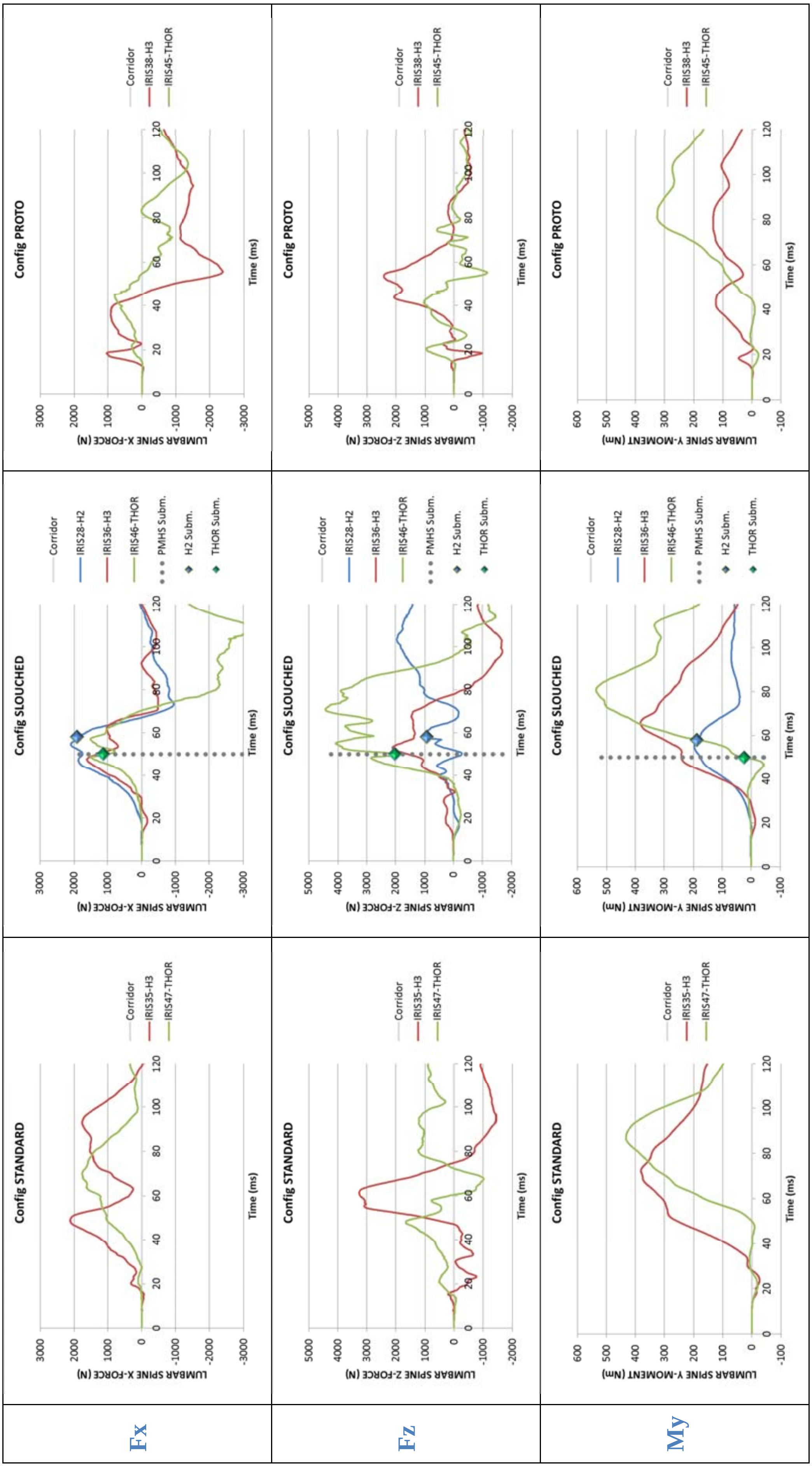

Fig. D 1. Dummies lumbar spine loads.